

Dynamin and the Actin Cytoskeleton Cooperatively Regulate Plasma Membrane Invagination by BAR and F-BAR Proteins

Toshiki Itoh,¹ Kai S. Erdmann,¹ Aurelien Roux,¹
Bianca Habermann,² Hauke Werner,^{1,3}
and Pietro De Camilli^{1,*}

¹Department of Cell Biology and
Howard Hughes Medical Institute
Boyer Center for Molecular Medicine
Yale University School of Medicine
New Haven, Connecticut 06510

²Scionics Computer Innovation, GmbH
c/o Max Planck Institute of Molecular Cell Biology
and Genetics
Pfotenhauerstrasse 108
01307 Dresden
Germany

Summary

Cell membranes undergo continuous curvature changes as a result of membrane trafficking and cell motility. Deformations are achieved both by forces extrinsic to the membrane as well as by structural modifications in the bilayer or at the bilayer surface that favor the acquisition of curvature. We report here that a family of proteins previously implicated in the regulation of the actin cytoskeleton also have powerful lipid bilayer-deforming properties via an N-terminal module (F-BAR) similar to the BAR domain. Several such proteins, like a subset of BAR domain proteins, bind to dynamin, a GTPase implicated in endocytosis and actin dynamics, via SH3 domains. The ability of BAR and F-BAR domain proteins to induce tubular invaginations of the plasma membrane is enhanced by disruption of the actin cytoskeleton and is antagonized by dynamin. These results suggest a close interplay between the mechanisms that control actin dynamics and those that mediate plasma membrane invagination and fission.

Introduction

Cell motility and intracellular membrane trafficking imply the occurrence of dynamic changes in the curvature of cell membranes. Studies carried out over the last few years have suggested a particularly important role in these changes of soluble cytosolic proteins that can directly and reversibly interact with the lipid bilayer (Farsad and De Camilli, 2003; Gallop and McMahon, 2005; Matsuoka et al., 1998; Sweitzer and Hinshaw, 1998; Takei et al., 1998). Some of these proteins deform membranes by directly penetrating their outer bilayer leaflet, thus creating an imbalance between the areas of the two leaflets that results in curvature acquisition (Farsad and De Camilli, 2003; Ford et al., 2002; Gallop

and McMahon, 2005; Lee et al., 2005). Other proteins are thought to bind the bilayer primarily via hydrophilic interfacial interactions and to deform it via their intrinsic curvature, or via their property to assemble into curved scaffolds, often referred to as “coats” (Bi et al., 2002; Peter et al., 2004; Rothman, 1994; Zhang and Hinshaw, 2001).

BAR (Bin-Amphiphysin-Rvs) domain proteins are a class of cytosolic proteins with membrane-deforming properties. The powerful membrane tubulation activity of these proteins was first identified for amphiphysin (Takei et al., 1999) and endophilin (Farsad et al., 2001; Ramjaun et al., 1997; Ringstad et al., 1997), two endocytic and signaling proteins that share similar domain organization, with an N-terminal BAR domain and a C-terminal SH3 domain. The BAR domain is the module that binds and deforms the membrane, often with the assistance of flanking sequences that enhance membrane association (Lee et al., 2002; Peter et al., 2004). The SH3 domain mediates interactions with other proteins, primarily the GTPase dynamin and the polyphosphoinositide phosphatase synaptojanin (McPherson et al., 1996; Ramjaun et al., 1997; Ringstad et al., 1997). Dynamin, also a membrane-deforming protein, participates in the generation, constriction, and fission of endocytic vesicle stalks (Hinshaw, 2000; Hinshaw and Schmid, 1995; Takei et al., 1995). Synaptojanin regulates the dephosphorylation of a pool of phosphatidylinositol 4,5-bisphosphate (PI(4,5)P₂) implicated in recruitment of dynamin, other endocytic factors, and actin (Cremona et al., 1999; McPherson et al., 1996; Sakisaka et al., 1997). Accordingly, major amphiphysin isoforms and the endophilins are localized at sites of endocytosis, where they contribute, together with dynamin, to the generation of membrane curvature at endocytic pits (Ramjaun et al., 1997; Ringstad et al., 1997; Takei et al., 1999).

More recently, structural and bioinformatics analyses have led to the identification of BAR domains in a wide variety of proteins (Habermann, 2004; Peter et al., 2004). Although these proteins differ from each other in domain organization and putative functions, they share the property of acting at sites of membrane dynamics, often at endocytic sites (Salazar et al., 2003; Soulet et al., 2005). Thus, the membrane-tubulating activity of their BAR domains, experimentally confirmed both in vitro and in vivo in some cases, is likely to play an important physiological role. An additional shared feature of many BAR domain proteins is that they play a direct or indirect role in the regulation of actin dynamics. For example, Rvs167, the homolog of amphiphysin and endophilin in *Saccharomyces cerevisiae*, participates both in endocytosis and actin function in this organism (Munn et al., 1995). Other BAR domain proteins contain binding sites or regulatory domains for Rho-GTPases or other actin regulatory proteins (Habermann, 2004; Peter et al., 2004). Dynamin itself has now been recognized as a regulator of actin function (Lee and De Camilli, 2002; McNiven et al., 2004; Orth et al., 2002; Schafer, 2004). Since growing evidence suggests an

*Correspondence: pietro.decamilli@yale.edu

³Present address: Department of Neurogenetics, Max-Planck-Institute of Experimental Medicine, Hermann Rein Strasse 3, D-37073 Goettingen, Germany.

involvement of actin in the fission reaction of endocytosis (Kaksonen et al., 2003; Merrifield et al., 2002, 2005; Yarar et al., 2005), the actin cytoskeleton may be an effector of dynamin in this reaction.

Syndapin/PACSIN is an endocytic and actin regulatory protein that binds dynamin, synaptojanin, and N-WASP via a C-terminal SH3 domain (Modregger et al., 2000; Qualmann et al., 1999). In addition to this domain, syndapin comprises an N-terminal FCH (Fes/CIP4 homology) domain, followed by a coiled-coil (CC) domain that shares some homology to the C-terminal half of the BAR domain, as recognized by its inclusion in a description of the BAR domain family (Peter et al., 2004). The FCH domain is present in a variety of proteins, including Nervous wreck (Nwk), WRP, ARHGAP4, FBP2, the protein tyrosine kinases Fer and Fes, Nostrin, CD2BP1, the yeast protein Cyk2p (Cdc15p in *S. pombe*), and the three closely related proteins Toca-1, FBP17 (Toca-2), and CIP4 (Toca-3) (Aspenstrom, 1997; Carnahan and Gould, 2003; Coyle et al., 2004; Greer, 2002; Ho et al., 2004; Li et al., 1998; Lippincott and Li, 1998; Soderling et al., 2002; Zimmermann et al., 2002). All of these proteins have been linked to actin by biochemical and/or genetic and functional studies. Toca-1, in particular, was identified as a critical factor in the Cdc42- and N-WASP-dependent activation of actin nucleation (Ho et al., 2004), and CIP4 and FBP17 are expected to have similar properties. One of them, FBP17, binds dynamin via a C-terminal SH3 domain and induces plasma membrane tubules in vivo, thus pointing to another link between FCH domain proteins and BAR domain proteins (Kamioka et al., 2004).

These observations prompted us to carry out a more systematic comparison between BAR domain- and FCH domain-containing proteins. Sequence comparisons and structural predictions suggested that the FCH domain, together with the CC region that typically follows this domain, define a protein module similar to the BAR domain, which we have named the F-BAR domain. BAR and F-BAR domain proteins share functional similarities, including a powerful membrane-deforming activity. The ability of BAR/F-BAR proteins to induce membrane tubulation in living cells is enhanced by disruption of the actin cytoskeleton with latrunculin and is counteracted by dynamin overexpression. Furthermore, reversal of latrunculin-induced tubulation is inhibited by mutant dynamin. These findings provide evidence for a link between proteins that deform membranes in endocytosis and actin regulatory mechanisms.

Results

The FCH Domain Is Part of a Larger Domain

Multiple sequence alignments of all mammalian FCH proteins as defined by the SMART database (<http://smart.embl-heidelberg.de>) revealed substantial sequence similarity not only among the FCH domains, but also among the adjacent regions, predicted to have a CC structure (Figure 1A). While identities and similarities were relatively low for the most distant members (16%–18% and 27%–45%, respectively), these entire regions (FCH + CC, ~300 amino acids) aligned well with minimal gaps, and several amino acid positions were conserved. A secondary structure prediction by

the Jnet program (Cuff and Barton, 2000) suggested a predominantly α -helical structure for the entire FCH-CC region. Further analysis aligned this entire amino acid sequence with the BAR domain and predicted, as in the case of the BAR domain, three distinct helices (Figure 1A). Thus, the FCH domain, although defined as a separate domain in databases, may be part of a larger, BAR domain-related module that includes the CC region. Based on these considerations, and supported by other results discussed in this paper (see below), we propose the definition of this module as “F-BAR domain,” which stands for “FCH and BAR.”

Domain Organization and Binding Properties of F-BAR and BAR Domain Proteins

A phylogenetic analysis of F-BAR and BAR domain proteins clearly reveals their relationship (Figure 1B). Interestingly, these two superfamilies share additional similarities besides the presence of these two related domains (Figure 1C). For example, F-BAR domains, like BAR domains (Habermann, 2004; Peter et al., 2004), are often found in proteins that also contain SH3 domains, regulatory modules for Rho family GTPases, or Rho family binding modules such as HR1 domains. Some modules, however, such as tyrosine kinase domains, are found only in F-BAR family proteins (Fes and Fer). In our studies of this protein superfamily, we concentrated on some of the F-BAR domain proteins also containing SH3 domains, i.e., the closest homologs of the founding members of BAR domain proteins.

A main binding partner of most SH3 domains present in BAR proteins is dynamin. Other binding partners include synaptojanin and N-WASP (McPherson et al., 1996; Ramjaun et al., 1997; Ringstad et al., 1997; Salazar et al., 2003). Likewise, the SH3 domains of two F-BAR proteins, syndapin (Qualmann et al., 1999) and FBP17 (Kamioka et al., 2004), were previously shown to bind dynamin. We tested whether this property is shared by the SH3 domain of other F-BAR domain family proteins. Indeed, pull-down assays from rat brain with the GST-SH3 domains of FBP17, CIP4, syndapin, and a GST fusion of the tandem SH3 domains of Nwk1 and Nwk2 demonstrated that the major protein band retained by all of these domains, as revealed by SDS-PAGE and Coomassie blue staining (Figure 1D), Western blotting (Figure S1; see the Supplemental Data available with this article online), and mass spectrometry of the gel band (data not shown), is dynamin. A much fainter band at ~75 kDa was identified as N-WASP (Figure S1), consistent with previous reports (Coyle et al., 2004; Ho et al., 2004; Kakimoto et al., 2004; Qualmann et al., 1999; Tian et al., 2000). Variable levels of synaptojanin were also detected by Western blotting in the bound material from all proteins (Figure S1). We conclude that, generally, binding specificities of SH3 domains of F-BAR and BAR domain proteins are similar. In additional studies, we focused on syndapin and members of the Toca-1/FBP17/CIP4 family.

F-BAR Domains Have Powerful Bilayer-Deforming Activity In Vitro

BAR domain proteins induce massive tubulation of liposomes in vitro (Farsad et al., 2001; Peter et al., 2004; Takei et al., 1999). We investigated whether this property

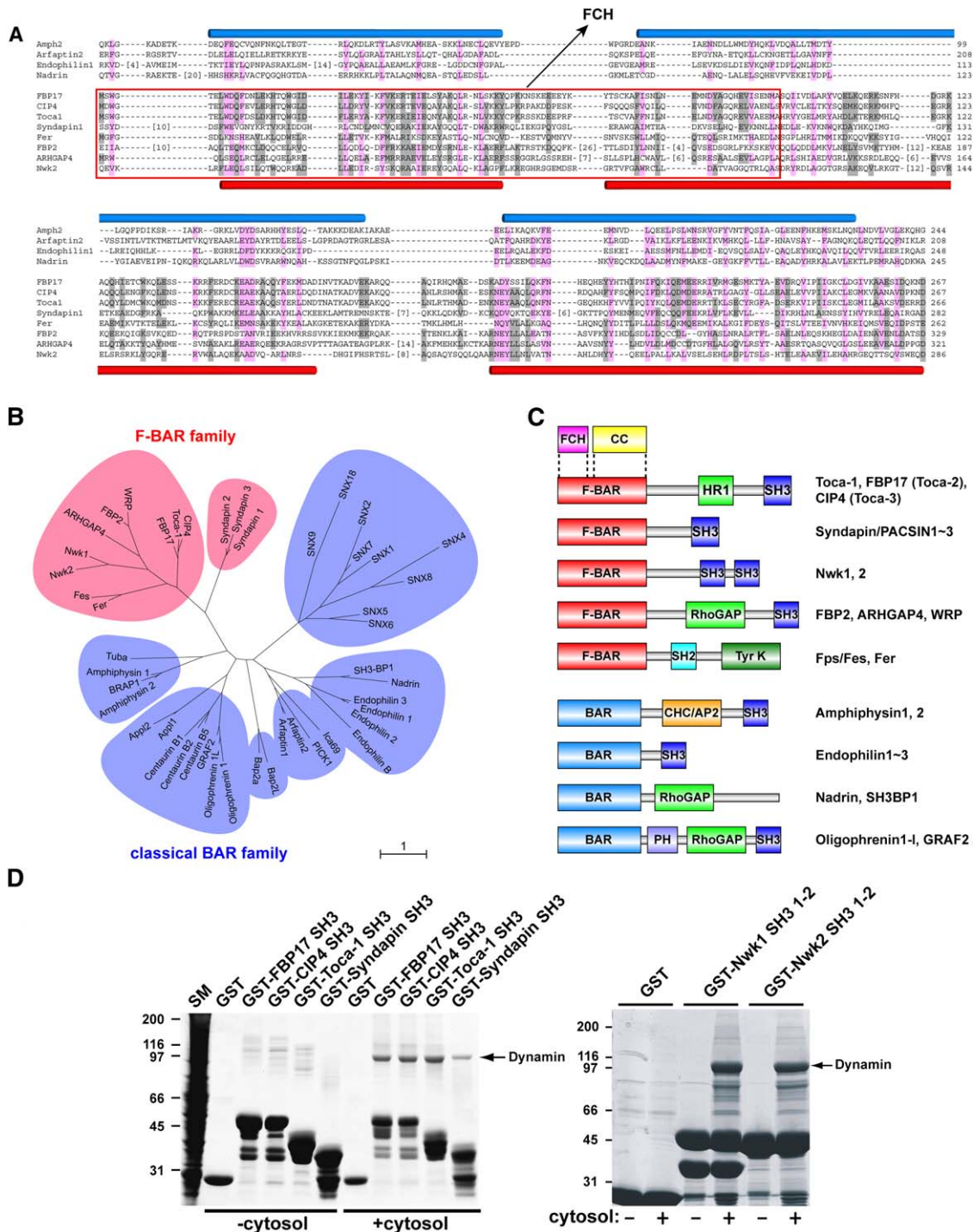


Figure 1. The FCH Domain Is Part of a BAR-like Domain

(A) Multiple sequence alignment of BAR and F-BAR domain proteins. Conserved residues in both domains are highlighted in magenta. The FCH domain is boxed in red, and its conserved residues are highlighted in gray. Secondary structural elements as predicted from the tertiary structure of amphiphysin or by the Jnet program with FBP17 sequence are shown above (BAR, blue) or below (F-BAR, red) the alignment. The alignment was done with ClustalX and was manually refined.

(B) Phylogenetic tree of the BAR/F-BAR domain family. Subfamilies of BAR and F-BAR domains are highlighted in light blue and pink, respectively.

(C) Diagram illustrating domain organization of a subset of BAR and F-BAR domain proteins.

(D) Pull-downs from rat brain cytosol with GST fusions of the SH3 domains of FBP17, CIP4, Toca-1, syndapin 1, Nwk1, and Nwk2. For Nwk proteins, which contain a tandem SH3 domain, both SH3 domains were included in the fusion protein. Coomassie blue staining of the bead fraction after incubation without and with brain cytosol are shown.

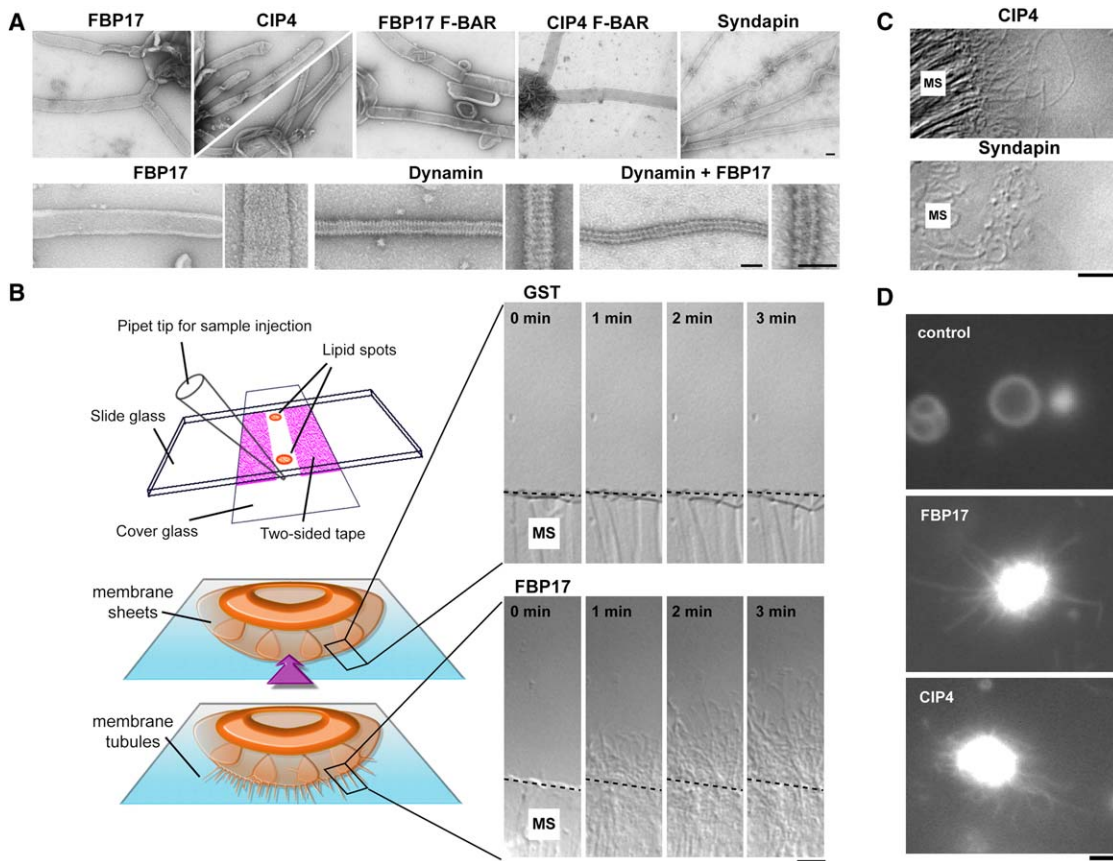


Figure 2. F-BAR Domains Tubulate Liposomes

(A) Negative staining electron microscopy. Upper panels: Liposomes were incubated with recombinant F-BAR-containing proteins or their isolated F-BAR domains. Lower panels: Liposomes were incubated either with FBP17 or with dynamin alone, or with both proteins together, as indicated. The presence of both proteins induced the reorganization of the FBP17-only- and dynamin-only-coated tubules into narrow tubules decorated by a striped coat (with thicker stripes than the dynamin-only coat) reminiscent of the hybrid amphiphysin/dynamin or endophilin/dynamin coat (Farsad et al., 2001; Takei et al., 1999). The scale bars are 100 nm.

(B) Left: Schematic drawing of the experimental system used to analyze the tubulation of lipid bilayers by differential interference contrast (DIC) microscopy as shown in the right field. Lipids are spotted in a small chamber between two glass surfaces, dried, and then rehydrated to generate bilayer sheets, typically composed of a few superimposed layers. Protein-containing solutions are added to the chamber during microscopic observation. The diagram of a lipid spot before and after application of a tubulating protein. Right: Time course analysis of edges of membrane sheets (MS) during the incubation with a control protein (top) or with FBP17 (bottom).

(C) Edges of lipid sheets after incubation with CIP4 and syndapin 1 as in (B), demonstrating the presence of lipid tubules.

(D) Liposomes were generated in suspension, then labeled with the fluorescence dye FM2-10 (top) and incubated with FBP17 (middle) or CIP4 (bottom). The scale bars are 5 μ m.

is also shared by F-BAR domain proteins. Recombinant FBP17, CIP4, syndapin, as well as the F-BAR domains of FBP17 (amino acids 1–284) or CIP4 (amino acids 1–284) were incubated with liposomes composed of a crude brain lipid extract (Folch fraction I). Negative staining electron microscopy of these preparations revealed that all of these proteins had a powerful tubulating activity (Figure 2A, upper panels). The diameter of F-BAR-induced tubules was somewhat variable and dependent on the experimental conditions (outer diameter between 40 and 200 nm). The polymerization property was suggested to play a role in the lipid-tubulating activity of BAR domains (Farsad and De Camilli, 2003; Peter et al., 2004). Interestingly, the F-BAR domain of FBP17, when incubated alone without liposomes, polymerized into long filaments (Figure S2).

In the presence of liposomes and dynamin, amphiphysin and endophilin generate narrow tubules of a highly uniform small diameter with a characteristic striped hy-

brid coat (thick stripes with a pitch of $\sim 20.2 \pm 1.5 \mu$ m) different from the striped coats generated by BAR proteins alone (very thin, tightly apposed stripes) or dynamin alone (thin stripes with a pitch of $\sim 13.2 \pm 0.5 \mu$ m [Farsad et al., 2001; Takei et al., 1999]). In a similar fashion, when incubations of FBP17 with liposomes were supplemented with dynamin, narrow tubules of a uniform diameter and with a striped coat resembling the amphiphysin/dynamin or endophilin/dynamin hybrid coat (thick stripes; pitch of $23.7 \pm 0.88 \mu$ m) were observed (Figure 2A, lower panels).

The powerful liposome tubulation activity of F-BAR proteins was confirmed by dynamic light microscopy-based assays. In a first assay, lipid droplets were first dried in a small chamber on a glass slide, and then hydrated to generate large bilayer sheets (Figure 2B). As shown by differential interference contrast (DIC) microscopy, the addition of all F-BAR domain proteins tested in this assay, namely FBP17, CIP4, and syndapin,

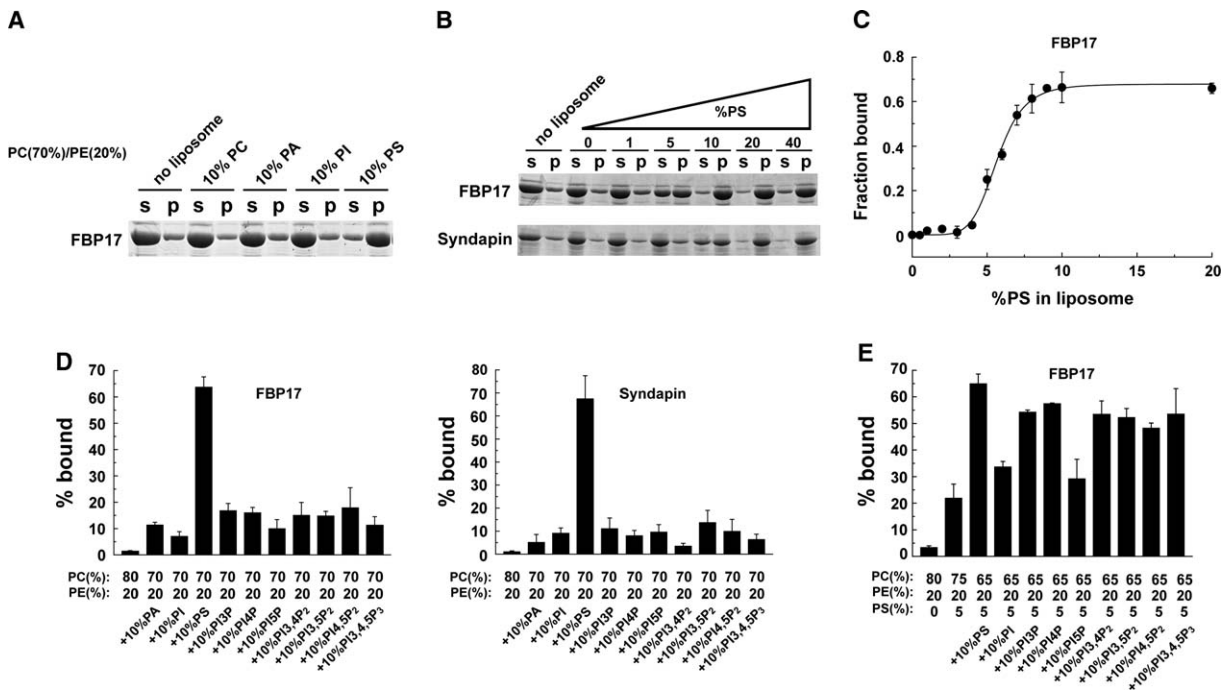


Figure 3. F-BAR Domains Bind to Phosphatidylserine and Phosphoinositides

(A and B) Liposome binding assays. FBP17 and syndapin 1 were incubated with liposomes composed of mixtures of 80% PC, 20% PE plus (with corresponding reduction in PC) 10% PA, PI, or PS, or variable percentages of PS and were then pelleted. Coomassie blue staining of SDS-PAGES of supernatant and pellet fractions are shown.

(C) Quantification of the results shown in (B).

(D) Liposomes were incubated with FBP17 and syndapin as described for (A) and (B), and results were expressed as percentages of bound protein. Liposomes were composed of either 80% PC and 20% PE (first bar), or by 70% PC, 20% PE, and 10% each of the phospholipids indicated. (E) Same as in (D), but in all conditions other than the first, 5% PC was replaced by 5% PS, and another 10% PC was replaced by 10% of the phospholipids indicated.

Error bars indicate standard error of the mean (SEM).

and the isolated F-BAR domains of FBP17 and CIP4 (final concentration of 1.0 mg/ml) induced massive formation of long lipid tubules at the membrane surface (Figures 2B and 2C). GST, used as a control, did not affect the shape of the membrane surface (Figure 2B; Movies S1 and S2). N- and C-terminal truncations of FBP17 revealed that the F-BAR domain (amino acids 1–284), was the minimal portion of the protein that could induce a tubulation similar to that induced by the full-length protein (data not shown). Furthermore, a point mutant of the FBP17 F-BAR domain (F-BAR^{L7E}) did not tubulate, but still bound liposomes in pull-down assays (data not shown), thus indicating that lipid binding is not sufficient for tubulation. In a second assay, proteins were incubated with liposomes (~5–10 μm in diameter) that had been preadsorbed to a glass slide and were labeled with the lipophilic fluorescent dye FM2-10. In this assay as well, all F-BAR domain proteins tested (FBP17, CIP4, and syndapin) induced formation of long (up to 20 μm) tubules (Figure 2D and data not shown). In conclusion, F-BAR domains, like BAR domains, have powerful membrane-tubulating activities.

F-BAR Domains Bind to Phosphatidylserine and Phosphoinositides

We next investigated the lipid binding profiles of F-BAR domain proteins. While FBP17 did not bind efficiently to synthetic liposomes composed of phosphatidyletha-

nolamine (PE) (20%) and phosphatidylcholine (PC) (80%), the presence of phosphatidylserine (PS), an acidic phospholipid concentrated at the cytosolic leaflet of the plasma membrane, strongly promoted binding (Figure 3A), with a maximal effect occurring at ~10% PS (Figures 3B and 3C). This effect was specific for PS, as other acidic phospholipids such as phosphatidic acid (PA) and phosphatidylinositol (PI), or phosphorylated versions of PI such as PI(3)P, PI(4)P, PI(5)P, PI(3,4)P₂, PI(3,5)P₂, PI(4,5)P₂, and PI(3,4,5)P₃, did not potentiate binding of the PC/PE mixture (Figure 3D). However, in the presence of PS (5%), PI(4,5)P₂ and several other phosphoinositides enhanced binding (Figure 3E). The binding properties of CIP4 were similar to those of FBP17 (data not shown). Syndapin binding was also strongly and specifically enhanced by PS (Figure 3D), but with a maximum binding at 20% of PS (Figure 3B). A plot of the binding efficiency as a function of the molar ratio of PS in the liposome revealed a sigmoidal curve with Hill coefficient values of 6.3 for FBP17 and 2.8 for syndapin 1 (Figure 3C and data not shown). In summary, these findings indicate a specific interaction between F-BAR domains and PS that is enhanced by phosphoinositides.

Overexpression of F-BAR Proteins Induces Membrane Tubulation In Vivo

We next investigated the membrane-deforming properties of F-BAR domain proteins in living cells. Studies of

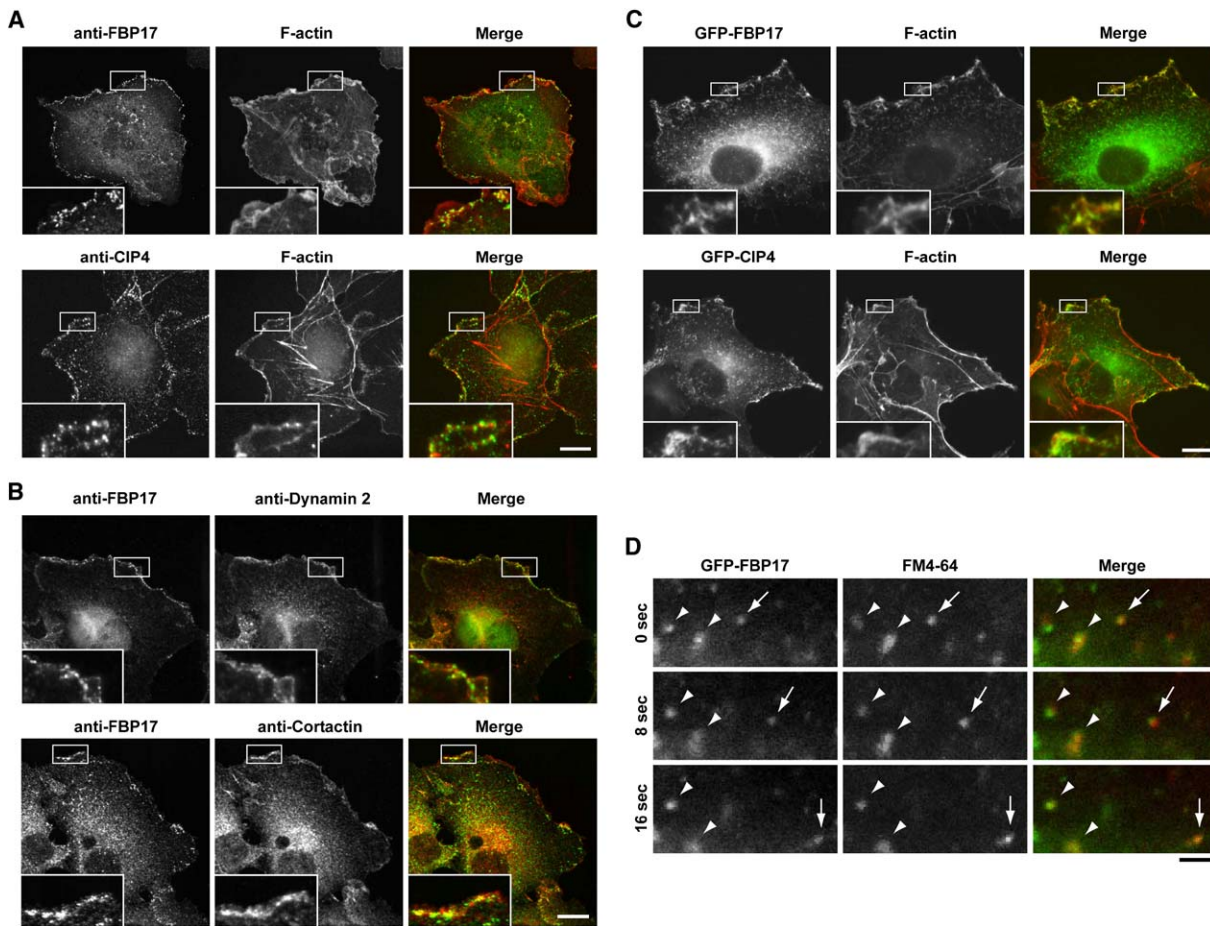


Figure 4. FBP17 and CIP4 Are Localized at Sites of Actin Nucleation

(A) Colocalization of endogenous F-BAR proteins with the actin cytoskeleton. COS-7 cells were fixed and immunostained with anti-FBP17 (green; upper panel) or anti-CIP4 (green; lower panel) antibody and rhodamine-phalloidin (red). (B) Colocalization of endogenous FBP17 (green) with dynamin 2 (red; upper panel) and cortactin (red; lower panel). (C) GFP-FBP17 (green; upper panel) and GFP-CIP4 (green; lower panel), when expressed at low levels in COS-7 cells, colocalize with F-actin (but not with stress fibers), as detected by phalloidin staining (red) after fixation. (D) Colocalization of FBP17 with endocytic membrane. Time course of intracellular vesicles of a cell transfected with GFP-FBP17 and incubated for 5 min with FM4-64. Two populations of vesicles are shown: stationary (arrowheads) and mobile (arrow) vesicles, both positive for GFP-FBP17 and FM4-64.

The scale bars are 10 μm in (A)–(C) and 2 μm in (D). Insets in (A), (B), and (C) show the regions boxed by white rectangles at higher magnification.

F-BAR proteins have linked them to the regulation of the actin cytoskeleton, and to N-WASP- and Cdc42-dependent actin nucleation in particular (Coyle et al., 2004; Ho et al., 2004; Kessels and Qualmann, 2002). Consistent with these previous observations, immunostaining of fixed COS-7 cells for endogenous FBP17 and CIP4 revealed their enrichment in cortical regions of the cell where they colocalized with F-actin (phalloidin staining), dynamin 2, and cortactin (Figures 4A and 4B). Similar results were obtained with low-level expression of GFP-FBP17 and GFP-CIP4 (Figure 4C). Dynamic color imaging of cells expressing low levels of RFP-FBP17 or RFP-CIP4 together with GFP fusions of actin, Arp3, and cortactin revealed that foci positive for F-BAR proteins were sites from which actin-positive structures nucleated (data not shown). In ruffles, they appeared to emerge from the edges of the cell periphery, and then to move centripetally. High-power observation revealed

that these fluorescent structures were often attached to vacuolar organelles, whose endocytic nature was demonstrated with fluorescent extracellular tracers such as FM4-64 (Figure 4D).

However, when expressed at higher levels, not only GFP-FBP17, as previously reported (Kamioka et al., 2004), but also GFP-CIP4 and to a lower extent GFP-Toca-1 induced membrane tubulation (Figure 5A and data not shown) that was similar to that induced by BAR proteins, such as amphiphysin (Lee et al., 2002; Peter et al., 2004) or endophilin 3 (see Figure S3). Similar effects were seen for transfections of their F-BAR domains alone (data not shown). Tubules induced by full-length proteins were positive for binding partners of the SH3 domains of these proteins, such as cotransfected dynamin 2 and synaptojanin 1 as well as for the cotransfected constitutive active form of Cdc42 (G12V) (Figure 5B), which binds the HR1 domain of Toca-1/FBP17/CIP4

(Ho et al., 2004) (Figure 5B). The continuity of these tubules with the cell surface was demonstrated by their accessibility to cholera toxin during an incubation on ice prior to cell fixation (Figure 5B). In cells in which tubulation was prominent, some rearrangement of the actin cytoskeleton was also observed, with the appearance of a pool of F-actin (phalloidin-positive) colocalized with the tubules (Figure 5C).

In view of the interaction of members of the Toca-1/ FBP17/CIP4 family with dynamin, we examined whether manipulations of their levels affect endocytosis. Indeed, endocytosis of transferrin was impaired in cells in which overexpression of any one member of the Toca-1/ FBP17/CIP4 family had produced intense tubulation, indicating a dominant-negative effect (Figure 5D). Furthermore, siRNA-mediated knockdown of FBP17 produced a significant reduction in the internalization of transferrin (~67% at 10 min) (Figure 5E). This effect was enhanced by the additional application of siRNAs specific for CIP4 and Toca-1 (~50% at 10 min) (Figure 5E). This treatment reduced the levels of CIP4 and Toca-1 as well (Figure 5E, upper panel).

Membrane Tubulation Is Counteracted by Dynamin

The relation of the F-BAR proteins under study to endocytosis (see above), and the role of dynamin in fission, prompted us to investigate whether tubulation was affected by manipulations of dynamin function. Analysis of cells expressing high levels of FBP17, CIP4, and endophilin 3—all proteins that induce massive tubulation and that bind dynamin—revealed that tubulation was much less prominent, often absent, if dynamin 2 was coexpressed in these cells (Figure 5F; quantification provided in Figure S4). This counteracting effect on tubulation was not observed by coexpression of mutant dynamin 2^{K44A} (Figure 5F). Furthermore, the inhibitory effect of cotransfected dynamin 2-GFP on FBP17-induced membrane tubulation was not observed in cells coexpressing either FBP17 lacking its SH3 domain (i.e., the dynamin binding domain) or the F-BAR domain alone (Figure 5F and data not shown). As expected, in these cells, dynamin 2 was not localized on the tubules (Figure 5F).

Membrane Tubulation Is Enhanced by Disruption of Actin Function

Given the many links of dynamin and of F-BAR proteins to actin, we also tested whether perturbation of actin function affected tubulation by these proteins. Cells expressing low levels of GFP-FBP17, GFP-CIP4, or GFP-Toca-1—i.e., levels not sufficient to induce membrane tubulation—were treated with Latrunculin B, an actin monomer-sequestering agent that blocks fast actin polymerization (Spector et al., 1983). Strikingly, numerous GFP-positive membrane tubules started to grow from GFP-positive spots within seconds after the addition of drug (Figures 6A–6C; Movies S3 and S4). Cytochalasin D (CytD), which binds the barbed ends of actin filaments and blocks their elongation, had the same effects (data not shown). Importantly, Latrunculin B also induced fluorescent tubules upon expression of GFP-syndapin (Figure 6B), an F-BAR domain protein that tubulates liposomes *in vitro* (Figure 2), but did not induce tubulation in living cells even when highly overexpressed (data not shown). Interestingly, even in cells not transfected with

any protein, Latrunculin B induced the formation of some short tubules that were positive for endogenous FBP17, as revealed by immunofluorescence (Figure 6D).

Similar results were obtained with BAR domain proteins. More specifically, under our experimental conditions, GFP fusions of muscle amphiphysin 2 (M-amphiphysin 2; Lee et al. [2002] and data not shown) and endophilin 3 (Figure S3) induced potent membrane tubulation when expressed in COS-7 cells, while GFP fusion of amphiphysin 1 and endophilin 1 did not (data not shown). However, the addition of Latrunculin B to cells expressing either one of the latter two proteins produced the emergence from the plasma membrane of several tubules enriched in these proteins (Figure 6E and data not shown; Movie S5).

Cooperation of Dynamin and Actin in Antagonizing Membrane Tubulation

The effect of Latrunculin B could have at least two main explanations. Latrunculin may facilitate plasma membrane invaginations by inducing the loss of an actin-based stabilizing scaffold under the plasma membrane that antagonizes membrane deformation. Another explanation, not mutually exclusive with the previous one, is that endocytic invaginations may not undergo fission, and may thus undergo elongation into tubules, due to a requirement for actin in fission.

To gain some insight into the role of impaired fission in the Latrunculin effect, we investigated whether the antagonistic action of dynamin overexpression on F-BAR protein-induced tubulation was affected by this drug. Indeed, Latrunculin B blocked the antagonistic action of dynamin 2-GFP on F-BAR-dependent membrane tubulation and promoted tubules formation even in cells expressing high levels of dynamin 2 (Figure 7A; Movie S6). These tubules were positive both for dynamin and for the F-BAR protein. Conversely, washout of the drug from these cells led to the rapid disappearance of the tubules (Figure 7B; Movies S7A and S7B). In contrast, tubules generated in cells expressing dynamin^{K44A} plus FBP17 did not undergo substantial changes (Figure 7B; Movie S8). Close inspection of tubule dynamics during their disappearance revealed “beading” and clear examples of fission (Figure 7C; Movies S7B, S9, and S10), in addition to progressive tubule collapse (Figure 7C; Movie S11). Collectively, our results demonstrate that dynamin-dependent fission plays a direct, although not exclusive, role in the negative control of overexpressed dynamin on membrane tubulation, and that dynamin acts in close concert with actin.

Discussion

This study reveals shared properties of members of a protein family that previous studies have shown to play an important role in the regulation of actin nucleation (Aspenstrom, 1997; Carnahan and Gould, 2003; Coyle et al., 2004; Greer, 2002; Ho et al., 2004; Li et al., 1998; Lippincott and Li, 1998; Soderling et al., 2002; Zimmermann et al., 2002). The defining feature of these proteins is the presence at their N terminus of a protein module, the F-BAR domain, which we show to be part of a special branch within the phylogenetic tree of BAR domains. We have focused here on some members of

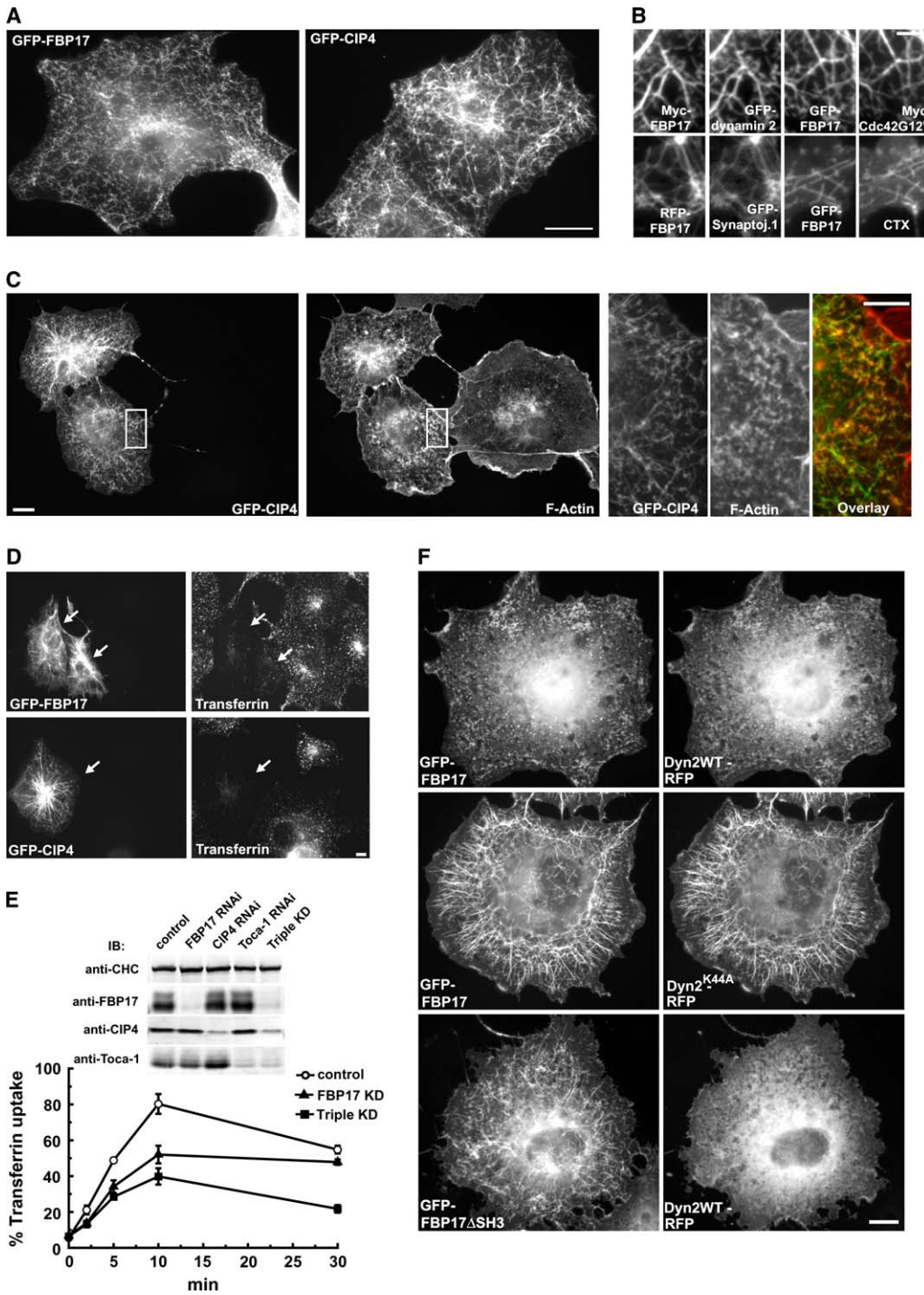


Figure 5. Effects of Manipulations of F-BAR Protein Expression on Membrane Tubulation and Endocytosis; Antagonistic Effect of Dynamin on Tubulation

(A) Fluorescent images of COS-7 cells that express high levels of GFP-FBP17 and GFP-CIP4, demonstrating the prominent membrane tubulation produced by these proteins.

(B) Details of cells cotransfected with GFP/RFP fusion proteins and Myc-tagged proteins, which have been fixed and processed for immunofluorescence analysis, are shown. Accessibility of the tubules to the extracellular space was demonstrated by incubation of cells with Cholera Toxin B-Alexa594 (CTX) on ice for 10 min followed by washing and fixation.

(C) Partial colocalization of actin with CIP4-induced tubules. Cells were transfected with GFP-CIP4, and F-actin was visualized after fixation with phalloidine-Texas red.

(D) Overexpression of members of the Toca-1/FBP17/CIP4 family impairs endocytosis of transferrin. COS-7 cells were transfected with the indicated GFP fusion proteins and incubated with Transferrin-Alexa594 for 10 min. After washing, cells were fixed and inspected by using fluorescence microscopy.

this protein family that bind dynamin. Like proteins with BAR domains, these proteins have membrane-deforming properties. Their intrinsic ability to induce tubular invaginations of the plasma membrane is antagonized by dynamin. This action of dynamin, which includes fission of the tubules, in turn requires the actin cytoskeleton, suggesting an important interplay of this GTPase with actin in membrane fission.

F-BAR Domains and BAR Domains

Portions of the F-BAR domain had been previously defined as distinct protein modules. The N-terminal part had been defined as the FCH domain, and the C-terminal part, predicted to have a CC organization, had been defined as the ARNEY domain (Coyle et al., 2004). The BAR-like structure of the CC subdomain in syndapin/PACSIN had also been noted (Peter et al., 2004). However, as we have shown here, the entire FCH and CC regions can be aligned with BAR domains, and they are predicted to have a similar secondary structure. In addition, gel filtration studies have indicated that F-BAR domains, like BAR domains, can form dimers (our unpublished data). Both F-BAR domains (this study) and BAR domains have a powerful bilayer-tubulating activity in vitro and can have strong tubulating activity in vivo. These activities require the entire F-BAR domain, because constructs that lack the FCH region could still bind lipids but not tubulate, both in vitro and in vivo (unpublished data and Kamioka et al., 2004). In some BAR domains, an amphipathic helix at the N-terminal side of the crystallographically defined BAR domain is thought to play a role in membrane tubulation (Farsad et al., 2001; Peter et al., 2004). While a similar helix may be present in some F-BAR proteins (our unpublished data), a clear definition of this issue awaits further structural studies.

F-BAR domain binding to phospholipid bilayers required the presence of the acidic phospholipid PS and was enhanced by phosphoinositides. Binding to PS was also observed for the BAR domain of amphiphysin (Takei et al., 1999), although the specificity of this requirement was not addressed for BAR proteins. Binding of F-BAR domains to PS-containing bilayers appeared to be multivalent, which may reflect either multiple binding sites for PS in the F-BAR domain or F-BAR domain oligomerization, as occurs for BAR domains. In fact, we observed F-BAR domain polymerization into filaments. This mechanism may be important, because the multimerization of the F-BAR domain was shown to correlate with its membrane-tubulating activity in vivo (Kamioka et al., 2004). PS was reported to be enriched in raft fractions of the plasma membrane (Pike et al., 2002), where Rac1 and Cdc42 GTPases also accumulate (del Pozo et al., 2004). Since F-BAR proteins bind and/or regulate Rho family GTPases (see below), PS and Rho

family GTPases may have synergistic function in the context of F-BAR domain protein biology. The additional increase in bilayer binding produced by phosphoinositides, including PI(4,5)P₂, is consistent with the role of PI(4,5)P₂ in the binding of endocytic factors and actin regulatory proteins to the plasma membrane (Wenk and De Camilli, 2004).

F-BAR/BAR Domain Proteins Are Part of an Actin Regulatory Network Linked to Endocytosis

The domain organization and protein interactions of F-BAR and BAR domain proteins reveals several common themes, in addition to the presence of a lipid bilayer-deforming module. Several BAR domains and F-BAR proteins bind small GTPases or contain regulatory modules for these enzymes, strongly suggesting their cooperation with small GTPases in the control of cellular processes that function at the membrane-cytosol interface (Haber-mann, 2004). One of these processes is the regulation of actin. In the case of the F-BAR proteins studied here, a particularly important link occurs with Cdc42 and with N-WASP (Coyle et al., 2004; Ho et al., 2004; Kakimoto et al., 2004; Qualmann et al., 1999; Tian et al., 2000), two proteins shown to participate in at least some form of endocytosis (Benesch et al., 2005; Garrett et al., 2000; Innocenti et al., 2005; Sabharanjak et al., 2002).

Another recurrent theme in a subset of BAR and F-BAR domain proteins is the presence of SH3 domains with similar binding specificities and preferences. The main interactors of BAR domain proteins are dynamin and synaptojanin, but at least some of them, such as Rvs167 in yeast (Bon et al., 2000) and Tuba in mammals (Salazar et al., 2003), also bind N-WASP/WAVE family members. Conversely, we show here that several F-BAR domain proteins previously shown to bind N-WASP via their SH3 domains, for example Toca-1 (Ho et al., 2004), CIP4 (Tian et al., 2000), and Nwk (Coyle et al., 2004), also bind dynamin and synaptojanin. All of these interactors participate in actin regulation and endocytosis. N-WASP is a major regulator of Arp2/3-mediated actin nucleation and is found at sites of endocytosis (Benesch et al., 2005; Merrifield et al., 2004). Synaptojanin regulates actin and endocytic proteins via its PI(4,5)P₂ dephosphorylating activity (Gad et al., 2000; Rusk et al., 2003; Sakisaka et al., 1997; Van Epps et al., 2004). Dynamin has a well established role in endocytosis (Koenig and Ikeda, 1989; Praefcke and McMahon, 2004; Sever, 2002; Sweitzer and Hinshaw, 1998; Takei et al., 1998), but has also been proposed to function as an actin regulatory protein (Lee and De Camilli, 2002; Orth et al., 2002; Schafer, 2004). Consistent with these observations, we showed that both overexpression and knockdown of proteins of the Toca/FBP17/CIP4 family impaired clathrin-mediated endocytosis of transferrin.

(E) Impaired transferrin endocytosis after knockdown (KD) of members of the Toca-1/FBP17/CIP4 family. Transfection of siRNAs as indicated into HeLa cells produces significant downregulation of the corresponding target proteins (Western blot). siRNA-treated cells were subjected to a transferrin-biotin based endocytosis assay as described in *Experimental Procedures*. Control represents HeLa cells treated with scrambled FBP17 siRNA. Error bars indicate standard error of the mean (SEM).

(F) GFP-FBP17-induced tubulation is antagonized by cooverexpressing dynamin 2. COS-7 cells were cotransfected under the same conditions with GFP-FBP17 or FBP17 lacking its SH3 domain (GFP-FBP17ΔSH3) and either dynamin 2 wild-type or dynamin 2^{K44A}. Representative pictures are shown.

The scale bars in (A), (B), the left and middle panels of (C), (D), and (F) are 10 μm, and the scale bar in the right panel of (C) is 5 μm.

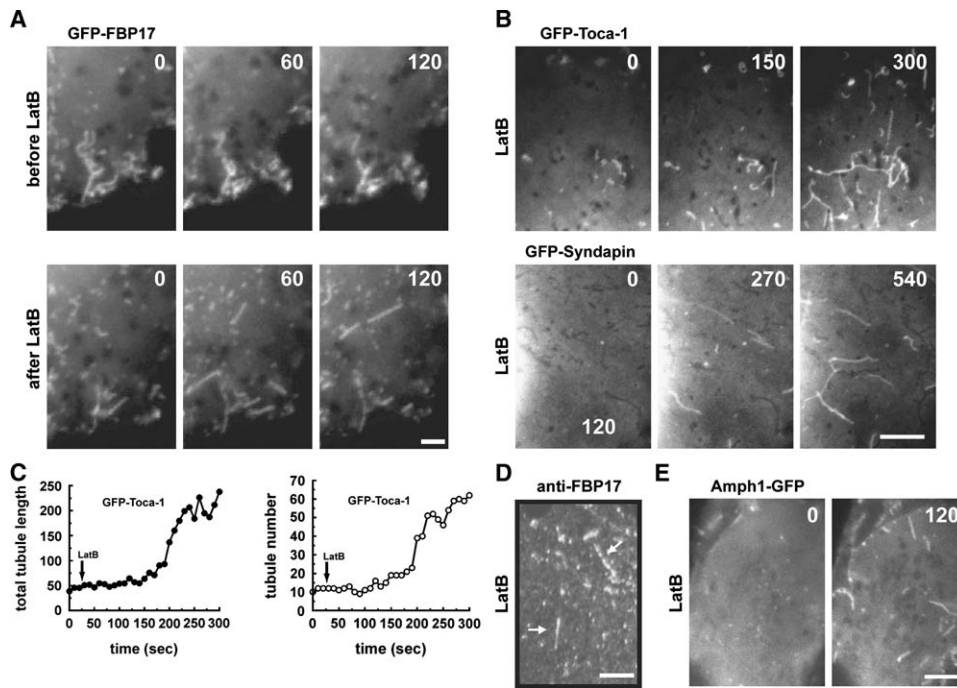


Figure 6. Inhibition of Actin Polymerization Induces Membrane Tubulation by F-BAR and BAR Proteins

(A) COS-7 cells were transfected with GFP-FBP17 (low level expression) and then imaged before and after the addition of Latrunculin B (1 μ M). Note the emergence of fluorescent tubules after Latrunculin B addition at the zero time of the bottom row.
 (B) Same as in (A), but with cells transfected with GFP-Toca-1 and GFP-syndapin.
 (C) Number of tubules and total tubule length, as a function of time, in a representative cell expressing GFP-Toca-1 and exposed to Latrunculin B.
 (D) Immunofluorescence for endogenous FBP17 in a cell exposed to Latrunculin B for 2 min.
 (E) Same as in (B), but in a cell expressing amphiphysin 1-GFP. Numbers indicate elapsed time in seconds.
 The scale bars are 2 μ m in (A) and 5 μ m in (B), (D), and (E).

BAR/F-BAR Proteins, Actin, and Fission

Our results provide new evidence for a role of BAR superfamily proteins in membrane deformation at the cell surface and in recruiting dynamin, a critical factor in the fission reaction of endocytosis. In addition, they point to an interplay between dynamin and the actin cytoskeleton in the fission reaction. Our study suggests that the formation of tubular invaginations of the plasma membrane could be the result of a balance between the bilayer-deforming and curvature-sensing properties of some membrane-associated proteins and at least two major mechanisms that counteract tubulation. One such counteracting mechanism is accounted for by dynamin, most likely because of its property to sever membrane tubules. Overexpression of dynamin prevents tubulation while dominant-negative dynamin allows tubulation to occur. The other counteracting mechanism is accounted for by the actin cytoskeleton, as indicated by experiments with Latrunculin B. Decreased membrane rigidity due to loss of the plasma membrane-associated actin-based cytoskeleton is likely to contribute to the tubule growth observed after Latrunculin B treatment. However, at least some of the actions of Latrunculin B may be due to an indirect effect on dynamin function. Thus, Latrunculin B blocked the antagonizing effect of dynamin overexpression on tubule formation, and such an effect was rapidly reestablished in cells expressing wild-type, but not mutant, dynamin-GFP after drug washout. In fact, this reversal of tubulation provided a striking visual demonstration of the role of dynamin in fission in

a living cell. We conclude that the function of dynamin and actin are tightly interconnected. More generally, our study demonstrates a critical functional relationship between factors that control plasma membrane curvature and fission and factors implicated in actin dynamics.

Experimental Procedures

Antibodies and Reagents

Polyclonal anti-FBP17 antibody was raised by immunizing rabbits with full-length FBP17 recombinant protein and was affinity purified. Polyclonal anti-synaptojanin 1 antibodies were described previously (McPherson et al., 1994). Anti-Toca-1 antibody was a kind gift from Marc Kirschner (Harvard Medical School). The following antibodies were purchased from commercial sources: monoclonal anti-dynamin 1 (hudy-1) from Upstate (Waltham, MA), polyclonal anti-N-WASP from Santa Cruz Biotechnology (Santa Cruz, CA), monoclonal anti-Myc from Sigma, monoclonal anti-CIP4 from BD Transduction Laboratories (San Jose, CA). Latrunculin B and cytochalasin D were purchased from Calbiochem (San Diego, CA). All fluorescent reagents (FM2-10, FM4-64, and AlexaFluor-488- and AlexaFluor-594-conjugated goat anti-rabbit or anti-mouse secondary antibodies) and Biotin-conjugated transferrin were purchased from Molecular Probes (Eugene, OR). Bovine brain lipid extract as well as purified phospholipids (PI, PA, PS, PE, PC) were purchased from Sigma. Brain polar lipid was purchased from Avanti Polar Lipids (Alabaster, AL). Phosphoinositides were purchased from Echelon Biosciences (Salt Lake City, UT).

DNA Constructs

Unless described otherwise, each cDNA fragment was subcloned into one of the following vectors: pGEX6P-1, 2 (Amersham Biosciences, Piscataway, NJ), pEGFP-N1, C1, or pMyc-CMV (Clontech, Mountain View, CA). cDNAs encoding human FBP17, CIP4, and

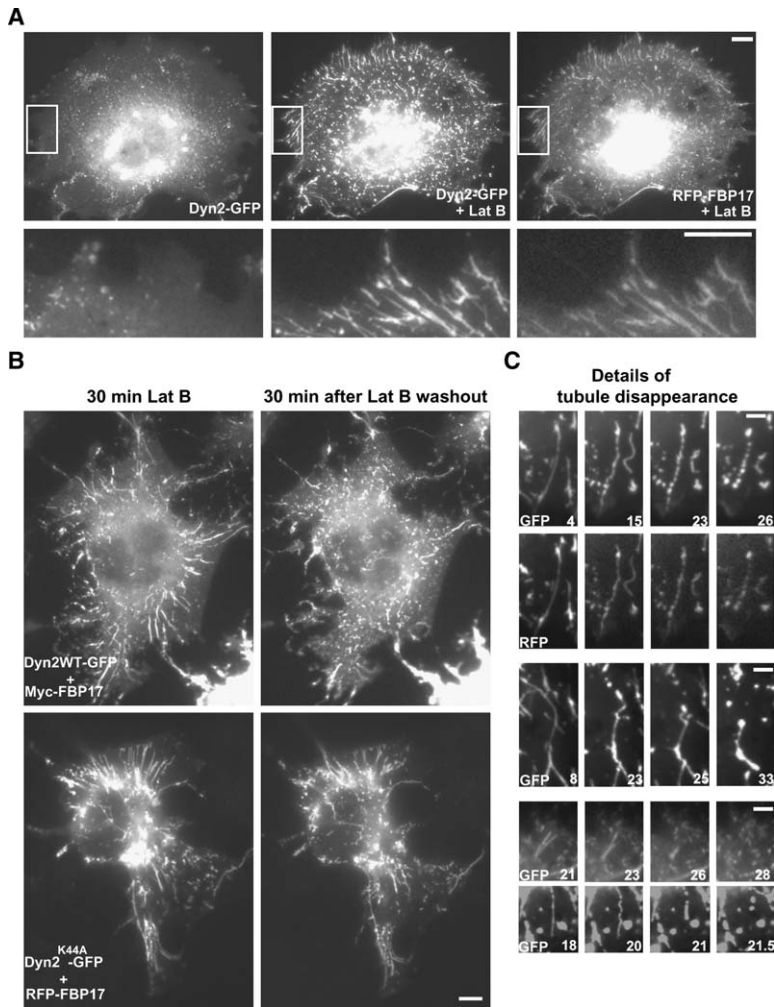


Figure 7. The Antagonistic Effect of Dynamin 2 on Tubule Formation Is Abolished by the Addition of Latrunculin B and Is Reestablished after Washout of the Drug

(A) Latrunculin B (1 μ M) was added to cells cotransfected with RFP-FBP17 and dynamin 2-GFP, and tubule growth was monitored by using fluorescence video microscopy. Latrunculin B-induced tubules are positive for both proteins. The lower panel shows the area enclosed by a rectangular in the upper panel at high magnification.

(B) COS-7 cells were transfected with Myc-FBP17 and either dynamin 2-GFP (upper panel) or RFP-FBP17 and dynamin 2^{K44A}-GFP (lower panel) and incubated with Latrunculin B for 30 min. After the washout of the drug, cells were monitored by video microscopy. The RFP and GFP signals overlapped throughout the experiment, but only the GFP signal is shown.

(C) Disappearance of tubules is mediated by beading, tubule collapse, and fission. The time course as seen in either the GFP or the RFP channel is shown. Numbers indicated time after Latrunculin B washout in minutes. The scale bars are 10 μ m in (A) and (B), and the scale bar is 5 μ m in (C).

endophilin 3 were obtained by PCR from a human brain cDNA by using primer sets designed on database sequences. The resulting FBP17 clone corresponded to rapostlin S (Kakimoto et al., 2004), a splice variant of rat FBP17 that lacks amino acids 330–390. The following constructs were kind gifts: cDNAs encoding human Toca-1 (H-form) (Ho et al., 2004) (from Marc Kirschner, Harvard University, Cambridge, MA), mouse syndapin 1/PACSIN 1 full-length cDNA in the pGEX3X vector (from Jan Modregger, our lab), rat dynamin 2 aa-GFP from Mark McNiven (Mayo Clinic, Rochester, MN) (Cao et al., 1998), rat dynamin 2-RFP and its K44A mutant from Roberto Zoncu (our lab), GFP-mouse cortactin from Marko Kaksonen (University of Helsinki, Finland) (Kaksonen et al., 2000), GFP-Arp3 from Dorothy Schafer (University of Virginia, Charlottesville, VA) (Schafer et al., 1998), Cdc42 (G12V) from Gianluca Cestra (our lab). The following partial constructs were PCR amplified or cut out by restriction enzyme digestion and subcloned into expression vectors: FBP17 F-BAR domain (amino acids 1–284), FBP17 SH3 domain (448–556), CIP4 F-BAR domain (1–284), CIP4 SH3 domain (529–601), Toca-1 SH3 domain (464–547), and endophilin 3 BAR domain (1–242). The tandem SH3 domains of mouse Nwk1 (485–657) and Nwk2 (459–620) (Coyle et al., 2004) were amplified by RT-PCR by using primers based on the sequences of mouse Fchsd1 and Fchsd2, respectively (Kato, 2004).

Bioinformatics

Sequence similarity searches were carried out by using the program PSI-BLAST (NCBI) against the nonredundant database (Altschul et al., 1997). Fold recognition of F-BAR proteins was carried out by using the 3D-PSSM server. Multiple sequence alignments were performed by using the program ClustalX (Jeanmougin et al., 1998) and

were subsequently manually refined. Phylogenetic analysis was carried out with the programs protdist and fitch from the Phylip package (Felsenstein, 1989). A total of 100 iterations were carried out for tree reconstruction.

Protein Biochemistry

Dynamin was purified from rat brain cytosol as described (Stowell et al., 1999). GST fusion proteins were bacterially expressed and purified according to the manufacturer's instructions. The GST tag was always removed by on-beads cleavage by using PreScission protease (Amersham Biosciences, Piscataway, NJ). GST pull-down assays from rat brains were performed as previously described (McPherson et al., 1994).

In Vitro Tubulation of Liposomes

Liposome preparation, in vitro tubulation reaction, negative staining, and electron microscopy were performed as previously described (Farsad et al., 2001; Takei et al., 1998), but with a modified buffer A (20 mM HEPES-NaOH [pH 7.4], 100 mM NaCl, 1 mM MgCl₂, 1 mM DTT). For live imaging of tubulation, the reaction was carried out in a small chamber as described (Roux et al., 2002). Liposomes (brain lipid extract, 1 mg/ml) were premixed with recombinant protein (1 mg/ml), injected into the chamber, and visualized by 10 μ M FM 2-10.

In Vitro Tubulation of Flat Membrane Sheets

Glass coverslips (22 mm \times 40 mm) were cleaned by sonication in 1% 7 \times (MP Biomed., Germany). After vigorous rinses and sonication in distilled water to remove any trace of detergent, they were washed once with 100% ethanol, kept in ethanol, and dried under a N₂ flux

just before use. To generate membrane sheets, two 1 μ l droplets of lipid solution (10 mg/ml Brain Polar Lipid Fraction in chloroform [Avanti Polar Lipids, Alabaster, AL]) were spotted on each coverslip and allowed to dry. In order to remove any trace of chloroform, coverslips were further dried under vacuum (0.2 milli-torr) for at least 1 hr, and were eventually kept several days under vacuum. Lipids were then rehydrated for 20–30 min in an incubator (37°C, 10% CO₂, 100% humidity), and a small chamber was built by placing the coverslip over a glass slide with strips of double-sided tape as spacers (see Figure 2A). Subsequently, lipids were fully rehydrated by injecting 15–20 μ l buffer A containing 0.1 mg/ml casein (C7078, Sigma, Switzerland) into the chamber. With the chamber mounted on the microscope stage (Axiovert 200 microscope [Carl Zeiss, Thornwood, NY]), 5 μ l protein solution was injected at one of its sides. The deformation of membrane sheets into tubules was recorded with a TM1400CL camera (JAI PULNIX, Sunnyvale, CA) and DVR software (Advanced Digital Vision, Natick, MA), which allowed normal video rate (30 fps) acquisition with high resolution (1300 \times 1024) in differential interference contrast (DIC) mode.

Liposome Binding Assay

Liposomes (1 mg/ml) were prepared in 100 μ l buffer A, incubated with 10 μ g protein for 15 min at room temperature, and sedimented by centrifugation at 16,000 \times g for 15 min. Bound and unbound fractions were separated by SDS-PAGE and visualized by Coomassie staining. Protein bands were quantified by using ImageJ software.

Cell Culture, Transfection, and Microscopy

COS-7 cells (ATCC, Rockville, MD) were cultured at 37°C and 5% CO₂ in Dulbecco's modified Eagle's medium supplemented with 10% fetal calf serum. Transfection was carried out by the Ca²⁺-phosphate method, and cells were observed after 16–24 hr. For immunofluorescence, cells were grown on coverslips, fixed with 4% formaldehyde (freshly prepared from paraformaldehyde), and processed by standard procedures. For live cell imaging, cells were grown and transfected on a 35 mm glass bottom dish (MatTek Corporation, Ashland, MA). The medium was replaced with 2 ml Krebs-Ringer solution (10 mM HEPES-NaOH [pH 7.4], 120 mM NaCl, 4.7 mM KCl, 1.2 mM CaCl₂, 0.7 mM MgSO₄, 10 mM glucose), and cells were imaged at room temperature on an Axiovert 200 microscope equipped with a MicroMax CCD camera (Princeton Instruments, Trenton, NJ). Images were collected and converted to AVI files by using MetaMorph software (Universal Imaging Corporation, Downingtown, PA). Files were further processed by using VirtualDub software (<http://VirtualDub.org>).

siRNA Protein Knockdown and Transferrin Uptake Assay

Small interfering RNAs (siRNAs) were designed by BLOCK-IT RNAi Designer (Invitrogen; <http://maidesigner.invitrogen.com/maiaexpress/>) and synthesized by Invitrogen Corp (Carlsbad, CA). Target sequences are as follows: FBP17, CCAACCUGAACGAAAUGAAUGAUUA; CIP4, CGAAGUGGAACAGCJUACGCCAAA; Toca-1, GCGAGAAGUUGUAGCAGAAGAAAUG; and control (scrambled FBP17 siRNA), CCAUCAGCAAGAAGUAAGUACAUA. HeLa cells were transfected with siRNAs at day 0 and day 2 according to manufacturer's instructions, and knockdown levels were assessed by Western blotting 48 hr after the second transfection. At the same time point, a transferrin uptake assay was carried out as described (Buss et al., 2001; Engqvist-Goldstein et al., 2004). For fluorescent transferrin uptake experiments on Toca-1/FBP17/CIP4 overexpression, cells were cultured on coverslips and incubated with Alexa-594-conjugated transferrin (30 μ g/ml; Molecular Probes) for 10 min. After acid stripping, cells were fixed with PFA.

Supplemental Data

Supplemental Data including 4 additional figures and 12 movies are available at <http://www.developmentalcell.com/cgi/content/full/9/6/791/DC1/>.

Acknowledgments

We thank Michele Solimena, Gilbert Di Paolo, Olivier Destaing, Karin Reinisch, Vinzenz Unger, and Adam Frost for discussion; Marc Py-paert and Mitsuko Hayashi for help with electron microscopy; and Marc Kirschner for the kind gift of anti-Toca-1 antibody. This work

was supported in part by grants from the National Institutes of Health (NS36251, DK54913, CA46128) and from the Yale Center for Genomics and Proteomics to P.D.C., by a postdoctoral Feodor-Lynen fellowship from the Alexander von Humboldt foundation to K.S.E., a European Molecular Biology Organization Long-Term fellowship and a Human Frontier Cross-Disciplinary fellowship to A.R., and a Japan Society for the Promotion of Science Postdoctoral fellowship for Research Abroad to T.I.

Received: June 15, 2005

Revised: September 17, 2005

Accepted: November 9, 2005

Published: December 5, 2005

References

- Altschul, S.F., Madden, T.L., Schaffer, A.A., Zhang, J., Zhang, Z., Miller, W., and Lipman, D.J. (1997). Gapped BLAST and PSI-BLAST: a new generation of protein database search programs. *Nucleic Acids Res.* 25, 3389–3402.
- Aspenstrom, P. (1997). A Cdc42 target protein with homology to the non-kinase domain of FER has a potential role in regulating the actin cytoskeleton. *Curr. Biol.* 7, 479–487.
- Benesch, S., Polo, S., Lai, F.P., Anderson, K.I., Stradal, T.E., Wehland, J., and Rottner, K. (2005). N-WASP deficiency impairs EGF internalization and actin assembly at clathrin-coated pits. *J. Cell Sci.* 118, 3103–3115.
- Bi, X., Corpina, R.A., and Goldberg, J. (2002). Structure of the Sec23/24-Sar1 pre-budding complex of the COPII vesicle coat. *Nature* 419, 271–277.
- Bon, E., Recordon-Navarro, P., Durrrens, P., Iwase, M., Toh, E.A., and Aigle, M. (2000). A network of proteins around Rvs167p and Rvs161p, two proteins related to the yeast actin cytoskeleton. *Yeast* 16, 1229–1241.
- Buss, F., Arden, S.D., Lindsay, M., Luzio, J.P., and Kendrick-Jones, J. (2001). Myosin VI isoform localized to clathrin-coated vesicles with a role in clathrin-mediated endocytosis. *EMBO J.* 20, 3676–3684.
- Cao, H., Garcia, F., and McNiven, M.A. (1998). Differential distribution of dynamin isoforms in mammalian cells. *Mol. Biol. Cell* 9, 2595–2609.
- Carnahan, R.H., and Gould, K.L. (2003). The PCH family protein, Cdc15p, recruits two F-actin nucleation pathways to coordinate cytokinetic actin ring formation in *Schizosaccharomyces pombe*. *J. Cell Biol.* 162, 851–862.
- Coyle, I.P., Koh, Y.H., Lee, W.C., Slind, J., Fergestad, T., Littleton, J.T., and Ganetzky, B. (2004). Nervous wreck, an SH3 adaptor protein that interacts with Wsp, regulates synaptic growth in *Drosophila*. *Neuron* 41, 521–534.
- Cremona, O., Di Paolo, G., Wenk, M.R., Luthi, A., Kim, W.T., Takei, K., Daniell, L., Nemoto, Y., Shears, S.B., Flavell, R.A., et al. (1999). Essential role of phosphoinositide metabolism in synaptic vesicle recycling. *Cell* 99, 179–188.
- Cuff, J.A., and Barton, G.J. (2000). Application of multiple sequence alignment profiles to improve protein secondary structure prediction. *Proteins* 40, 502–511.
- del Pozo, M.A., Alderson, N.B., Kiosses, W.B., Chiang, H.H., Anderson, R.G., and Schwartz, M.A. (2004). Integrins regulate Rac targeting by internalization of membrane domains. *Science* 303, 839–842.
- Engqvist-Goldstein, A.E., Zhang, C.X., Carreno, S., Barroso, C., Heuser, J.E., and Drubin, D.G. (2004). RNAi-mediated Hip1R silencing results in stable association between the endocytic machinery and the actin assembly machinery. *Mol. Biol. Cell* 15, 1666–1679.
- Farsad, K., and De Camilli, P. (2003). Mechanisms of membrane deformation. *Curr. Opin. Cell Biol.* 15, 372–381.
- Farsad, K., Ringstad, N., Takei, K., Floyd, S.R., Rose, K., and De Camilli, P. (2001). Generation of high curvature membranes mediated by direct endophilin bilayer interactions. *J. Cell Biol.* 155, 193–200.
- Felsenstein, J. (1989). PHYLIP - Phylogeny Inference Package (Version 3.2). *Cladistics* 5, 164–166.

- Ford, M.G., Mills, I.G., Peter, B.J., Vallis, Y., Praefcke, G.J., Evans, P.R., and McMahon, H.T. (2002). Curvature of clathrin-coated pits driven by epsin. *Nature* 419, 361–366.
- Gad, H., Ringstad, N., Low, P., Kjaerulf, O., Gustafsson, J., Wenk, M., Di Paolo, G., Nemoto, Y., Crun, J., Ellisman, M.H., et al. (2000). Fission and uncoating of synaptic clathrin-coated vesicles are perturbed by disruption of interactions with the SH3 domain of endophilin. *Neuron* 27, 301–312.
- Gallop, J.L., and McMahon, H.T. (2005). BAR domains and membrane curvature: bringing your curves to the BAR. *Biochem. Soc. Symp.* 72, 223–231.
- Garrett, W.S., Chen, L.M., Kroschewski, R., Ebersold, M., Turley, S., Trombetta, S., Galan, J.E., and Mellman, I. (2000). Developmental control of endocytosis in dendritic cells by Cdc42. *Cell* 102, 325–334.
- Greer, P. (2002). Closing in on the biological functions of Fps/Fes and Fer. *Nat. Rev. Mol. Cell Biol.* 3, 278–289.
- Habermann, B. (2004). The BAR-domain family of proteins: a case of bending and binding? *EMBO Rep.* 5, 250–255.
- Hinshaw, J.E. (2000). Dynamin and its role in membrane fission. *Annu. Rev. Cell Dev. Biol.* 16, 483–519.
- Hinshaw, J.E., and Schmid, S.L. (1995). Dynamin self-assembles into rings suggesting a mechanism for coated vesicle budding. *Nature* 374, 190–192.
- Ho, H.Y., Rohatgi, R., Lebensohn, A.M., Le, M., Li, J., Gygi, S.P., and Kirschner, M.W. (2004). Toca-1 mediates Cdc42-dependent actin nucleation by activating the N-WASP-WIP complex. *Cell* 118, 203–216.
- Innocenti, M., Gerboth, S., Rottner, K., Lai, F.P., Hertzog, M., Stradal, T.E., Frittoli, E., Didry, D., Polo, S., Disanza, A., et al. (2005). Abi1 regulates the activity of N-WASP and WAVE in distinct actin-based processes. *Nat. Cell Biol.* 7, 969–976.
- Jeanmougin, F., Thompson, J.D., Gouy, M., Higgins, D.G., and Gibson, T.J. (1998). Multiple sequence alignment with Clustal X. *Trends Biochem. Sci.* 23, 403–405.
- Kakimoto, T., Katoh, H., and Negishi, M. (2004). Identification of splicing variants of Rapostin, a novel RND2 effector that interacts with neural Wiskott-Aldrich syndrome protein and induces neurite branching. *J. Biol. Chem.* 279, 14104–14110.
- Kaksonen, M., Peng, H.B., and Rauvala, H. (2000). Association of cortactin with dynamic actin in lamellipodia and on endosomal vesicles. *J. Cell Sci.* 113, 4421–4426.
- Kaksonen, M., Sun, Y., and Drubin, D.G. (2003). A pathway for association of receptors, adaptors, and actin during endocytic internalization. *Cell* 115, 475–487.
- Kamioka, Y., Fukuhara, S., Sawa, H., Nagashima, K., Masuda, M., Matsuda, M., and Mochizuki, N. (2004). A novel dynamin-associating molecule, formin-binding protein 17, induces tubular membrane invaginations and participates in endocytosis. *J. Biol. Chem.* 279, 40091–40099.
- Katoh, M. (2004). Identification and characterization of human FCHSD1 and FCHSD2 genes in silico. *Int. J. Mol. Med.* 13, 749–754.
- Kessels, M.M., and Qualmann, B. (2002). Syndapins integrate N-WASP in receptor-mediated endocytosis. *EMBO J.* 21, 6083–6094.
- Koenig, J.H., and Ikeda, K. (1989). Disappearance and reformation of synaptic vesicle membrane upon transmitter release observed under reversible blockage of membrane retrieval. *J. Neurosci.* 9, 3844–3860.
- Lee, E., and De Camilli, P. (2002). Dynamin at actin tails. *Proc. Natl. Acad. Sci. USA* 99, 161–166.
- Lee, E., Marcucci, M., Daniell, L., Pypaert, M., Weisz, O.A., Ochoa, G.C., Farsad, K., Wenk, M.R., and De Camilli, P. (2002). Amphiphysin 2 (Bin1) and T-tubule biogenesis in muscle. *Science* 297, 1193–1196.
- Lee, M.C., Orci, L., Hamamoto, S., Futai, E., Ravazzola, M., and Schekman, R. (2005). Sar1p N-terminal helix initiates membrane curvature and completes the fission of a COPII vesicle. *Cell* 122, 605–617.
- Li, J., Nishizawa, K., An, W., Hussey, R.E., Lialios, F.E., Salgia, R., Sunder-Plassmann, R., and Reinherz, E.L. (1998). A cdc15-like adaptor protein (CD2BP1) interacts with the CD2 cytoplasmic domain and regulates CD2-triggered adhesion. *EMBO J.* 17, 7320–7336.
- Lippincott, J., and Li, R. (1998). Dual function of Cyk2, a cdc15/PSTPIP family protein, in regulating actomyosin ring dynamics and septin distribution. *J. Cell Biol.* 143, 1947–1960.
- Matsuoka, K., Orci, L., Amherdt, M., Bednarek, S.Y., Hamamoto, S., Schekman, R., and Yeung, T. (1998). COPII-coated vesicle formation reconstituted with purified coat proteins and chemically defined liposomes. *Cell* 93, 263–275.
- McNiven, M.A., Baldassarre, M., and Buccione, R. (2004). The role of dynamin in the assembly and function of podosomes and invadopodia. *Front. Biosci.* 9, 1944–1953.
- McPherson, P.S., Takei, K., Schmid, S.L., and De Camilli, P. (1994). p145, a major Grb2-binding protein in brain, is co-localized with dynamin in nerve terminals where it undergoes activity-dependent dephosphorylation. *J. Biol. Chem.* 269, 30132–30139.
- McPherson, P.S., Garcia, E.P., Slepnev, V.I., David, C., Zhang, X., Grabs, D., Sossin, W.S., Bauerfeind, R., Nemoto, Y., and De Camilli, P. (1996). A presynaptic inositol-5-phosphatase. *Nature* 379, 353–357.
- Merrifield, C.J., Feldman, M.E., Wan, L., and Almers, W. (2002). Imaging actin and dynamin recruitment during invagination of single clathrin-coated pits. *Nat. Cell Biol.* 4, 691–698.
- Merrifield, C.J., Qualmann, B., Kessels, M.M., and Almers, W. (2004). Neural Wiskott Aldrich Syndrome Protein (N-WASP) and the Arp2/3 complex are recruited to sites of clathrin-mediated endocytosis in cultured fibroblasts. *Eur. J. Cell Biol.* 83, 13–18.
- Merrifield, C.J., Perrais, D., and Zenisek, D. (2005). Coupling between clathrin-coated-pit invagination, cortactin recruitment, and membrane scission observed in live cells. *Cell* 121, 593–606.
- Modregger, J., Ritter, B., Witter, B., Paulsson, M., and Plomann, M. (2000). All three PACSIN isoforms bind to endocytic proteins and inhibit endocytosis. *J. Cell Sci.* 113, 4511–4521.
- Munn, A.L., Stevenson, B.J., Geli, M.J., and Riezman, H. (1995). end5, end6, and end7: mutations that cause actin delocalization and block the internalization step of endocytosis in *Saccharomyces cerevisiae*. *Mol. Biol. Cell* 6, 1721–1742.
- Orth, J.D., Krueger, E.W., Cao, H., and McNiven, M.A. (2002). The large GTPase dynamin regulates actin comet formation and movement in living cells. *Proc. Natl. Acad. Sci. USA* 99, 167–172.
- Peter, B.J., Kent, H.M., Mills, I.G., Vallis, Y., Butler, P.J., Evans, P.R., and McMahon, H.T. (2004). BAR domains as sensors of membrane curvature: the amphiphysin BAR structure. *Science* 303, 495–499.
- Pike, L.J., Han, X., Chung, K.N., and Gross, R.W. (2002). Lipid rafts are enriched in arachidonic acid and plasmenylethanolamine and their composition is independent of caveolin-1 expression: a quantitative electrospray ionization/mass spectrometric analysis. *Biochemistry* 41, 2075–2088.
- Praefcke, G.J., and McMahon, H.T. (2004). The dynamin superfamily: universal membrane tubulation and fission molecules? *Nat. Rev. Mol. Cell Biol.* 5, 133–147.
- Qualmann, B., Roos, J., DiGregorio, P.J., and Kelly, R.B. (1999). Syndapin I, a synaptic dynamin-binding protein that associates with the neural Wiskott-Aldrich syndrome protein. *Mol. Biol. Cell* 10, 501–513.
- Ramjaun, A.R., Micheva, K.D., Bouchelet, I., and McPherson, P.S. (1997). Identification and characterization of a nerve terminal-enriched amphiphysin isoform. *J. Biol. Chem.* 272, 16700–16706.
- Ringstad, N., Nemoto, Y., and De Camilli, P. (1997). The SH3p4/Sh3p8/SH3p13 protein family: binding partners for synaptotagmin and dynamin via a Grb2-like Src homology 3 domain. *Proc. Natl. Acad. Sci. USA* 94, 8569–8574.
- Rothman, J.E. (1994). Mechanisms of intracellular protein transport. *Nature* 372, 55–63.
- Roux, A., Cappello, G., Cartaud, J., Prost, J., Goud, B., and Basseau, P. (2002). A minimal system allowing tubulation with molecular motors pulling on giant liposomes. *Proc. Natl. Acad. Sci. USA* 99, 5394–5399.

- Rusk, N., Le, P.U., Mariggio, S., Guay, G., Lurisci, C., Nabi, I.R., Corda, D., and Symons, M. (2003). Synaptojanin 2 functions at an early step of clathrin-mediated endocytosis. *Curr. Biol.* *13*, 659–663.
- Sabharanjak, S., Sharma, P., Parton, R.G., and Mayor, S. (2002). GPI-anchored proteins are delivered to recycling endosomes via a distinct cdc42-regulated, clathrin-independent pinocytic pathway. *Dev. Cell* *2*, 411–423.
- Sakisaka, T., Itoh, T., Miura, K., and Takenawa, T. (1997). Phosphatidylinositol 4,5-bisphosphate phosphatase regulates the rearrangement of actin filaments. *Mol. Cell. Biol.* *17*, 3841–3849.
- Salazar, M.A., Kwiatkowski, A.V., Pellegrini, L., Cestra, G., Butler, M.H., Rossman, K.L., Serna, D.M., Sondek, J., Gertler, F.B., and De Camilli, P. (2003). Tuba, a novel protein containing bin/amphiphysin/Rvs and Dbl homology domains, links dynamin to regulation of the actin cytoskeleton. *J. Biol. Chem.* *278*, 49031–49043.
- Schafer, D.A. (2004). Regulating actin dynamics at membranes: a focus on dynamin. *Traffic* *5*, 463–469.
- Schafer, D.A., Welch, M.D., Machesky, L.M., Bridgman, P.C., Meyer, S.M., and Cooper, J.A. (1998). Visualization and molecular analysis of actin assembly in living cells. *J. Cell Biol.* *143*, 1919–1930.
- Sever, S. (2002). Dynamin and endocytosis. *Curr. Opin. Cell Biol.* *14*, 463–467.
- Soderling, S.H., Binns, K.L., Wayman, G.A., Davee, S.M., Ong, S.H., Pawson, T., and Scott, J.D. (2002). The WRP component of the WAVE-1 complex attenuates Rac-mediated signalling. *Nat. Cell Biol.* *4*, 970–975.
- Soulet, F., Yarar, D., Leonard, M., and Schmid, S.L. (2005). SNX9 regulates dynamin assembly and is required for efficient clathrin-mediated endocytosis. *Mol. Biol. Cell* *16*, 2058–2067.
- Spector, I., Shochet, N.R., Kashman, Y., and Groweiss, A. (1983). Latrunculins: novel marine toxins that disrupt microfilament organization in cultured cells. *Science* *219*, 493–495.
- Stowell, M.H., Marks, B., Wigge, P., and McMahon, H.T. (1999). Nucleotide-dependent conformational changes in dynamin: evidence for a mechanochemical molecular spring. *Nat. Cell Biol.* *1*, 27–32.
- Sweitzer, S.M., and Hinshaw, J.E. (1998). Dynamin undergoes a GTP-dependent conformational change causing vesiculation. *Cell* *93*, 1021–1029.
- Takei, K., McPherson, P.S., Schmid, S.L., and De Camilli, P. (1995). Tubular membrane invaginations coated by dynamin rings are induced by GTP-gamma S in nerve terminals. *Nature* *374*, 186–190.
- Takei, K., Haucke, V., Slepnev, V., Farsad, K., Salazar, M., Chen, H., and De Camilli, P. (1998). Generation of coated intermediates of clathrin-mediated endocytosis on protein-free liposomes. *Cell* *94*, 131–141.
- Takei, K., Slepnev, V.I., Haucke, V., and De Camilli, P. (1999). Functional partnership between amphiphysin and dynamin in clathrin-mediated endocytosis. *Nat. Cell Biol.* *1*, 33–39.
- Tian, L., Nelson, D.L., and Stewart, D.M. (2000). Cdc42-interacting protein 4 mediates binding of the Wiskott-Aldrich syndrome protein to microtubules. *J. Biol. Chem.* *275*, 7854–7861.
- Van Epps, H.A., Hayashi, M., Lucast, L., Stearns, G.W., Hurley, J.B., De Camilli, P., and Brockerhoff, S.E. (2004). The zebrafish nrc mutant reveals a role for the polyphosphoinositide phosphatase synaptojanin 1 in cone photoreceptor ribbon anchoring. *J. Neurosci.* *24*, 8641–8650.
- Wenk, M.R., and De Camilli, P. (2004). Protein-lipid interactions and phosphoinositide metabolism in membrane traffic: insights from vesicle recycling in nerve terminals. *Proc. Natl. Acad. Sci. USA* *101*, 8262–8269.
- Yarar, D., Waterman-Storer, C.M., and Schmid, S.L. (2005). A dynamic actin cytoskeleton functions at multiple stages of clathrin-mediated endocytosis. *Mol. Biol. Cell* *16*, 964–975.
- Zhang, P., and Hinshaw, J.E. (2001). Three-dimensional reconstruction of dynamin in the constricted state. *Nat. Cell Biol.* *3*, 922–926.
- Zimmermann, K., Opitz, N., Dedio, J., Renne, C., Muller-Esterl, W., and Oess, S. (2002). NOSTRIN: a protein modulating nitric oxide release and subcellular distribution of endothelial nitric oxide synthase. *Proc. Natl. Acad. Sci. USA* *99*, 17167–17172.